IEEE Access
Multidisciplinary | Rapid Review | Open Access Journal

SPECIAL SECTION ON NEURAL ENGINEERING INFORMATICS

Received July 8, 2019, accepted August 1, 2019, date of publication August 8, 2019, date of current version August 22, 2019.

Digital Object Identifier 10.1109/ACCESS.2019.2933990

Relational Network of People Constructed on the Basis of Similarity of Brain Activities

RYOICHI SHINKUMA[1], (Senior Member, IEEE), SATOSHI NISHIDA[2], MASATAKA KADO[3], NAOYA MAEDA[3], AND SHINJI NISHIMOTO[2]

[1]Graduate School of Informatics, Kyoto University, Kyoto 606-8501, Japan
[2]Center for Information and Neural Networks (CiNet), National Institute of Information and Communications Technology (NICT), Suita 565-0871, Japan
[3]NTT DATA Corporation, Tokyo 135-8671, Japan

Corresponding author: Ryoichi Shinkuma (shinkuma@i.kyoto-u.ac.jp)

This work was supported in part by the Japan Science and Technology Agency as PRESTO under Grant JPMJPR1854, in part by the Japan Society for the Promotion of Science as KAKENHI under Grant 18K18141, and in part by the Tateishi Science and Technology Promotion Foundation under Grant 2191025.

ABSTRACT The relational network of people (RNP) model has been attracting the interest of not only researchers but also industrial engineers. RNP can be constructed from friend lists in online social networking services (SNSs) and from inter-contact logs between individuals. One of the killer applications of RNP is the prediction of user demands, which is key to maximizing user satisfaction in content delivery services such as video streaming and video advertising. It is well known that an RNP representing social closeness between individuals (a so-called social network) can estimate user preferences simply, as we expect that people close to each other will have similar preferences. However, although there are many metrics that enable the social closeness between individuals to be measured, it is unclear which metric is best suited for individual services. Therefore, this paper introduces a new approach based on brain imaging. Brain imaging using functional Magnetic Resonance Imaging (fMRI) is powerful because it enables us to directly observe how a video content stimulates the brains of individual people. We propose a brain imaging-based RNP that represents the similarity of video-evoked brain activities between people as a network graph. We show an application scenario featuring predictive content delivery using the proposed RNP in which, when a user shows interest in a video content in some way, other users close to him or her can be expected to also be interested in it because their brain activities are correlated. Through numerical evaluation using multiple real datasets obtained by fMRI, we demonstrate that the proposed RNP is generalizable across brain imaging results for different sets of video content, thus suggesting that brain imaging data can be used to robustly generate RNP for utilization as a powerful tool for estimating user preferences.

INDEX TERMS Relational graph of people, brain imaging, fMRI.

I. INTRODUCTION

The relational network of people (RNP) model has been attracting the interest of not only researchers but also industrial engineers. RNP can be constructed from friend lists in online social networking services (SNSs) and from inter-contact logs between individuals and is managed by using a database as structured data [1]. One of the killer applications of RNP is the prediction of user demands, which is key to maximizing user satisfaction in content delivery services such as video streaming and video advertising.

The video content delivery market, which includes video streaming and video advertising, has grown exponentially over the last decade and is continuing to grow. According to Statista [2], revenue in the video streaming segment amounts to US $24,837 m in 2019. It is forecast that the revenue will show an annual growth rate (CAGR 2019–2023) of 3.2%, resulting in a market volume of US $28,190 m by 2023. User penetration is 14.6% in 2019 and is expected to hit 16.3% by 2023. Globally, most revenue is generated in the United States (US $11,420 m in 2019). As for the video advertising segment, it amounts to US $35,594 m in 2019. It is forecast that the revenue will show an annual growth rate (CAGR 2019–2023) of 13.4%, resulting in a market volume of US $58,764 m by 2023.

It is well known that an RNP representing social closeness between individuals (a so-called social network) can estimate user preferences simply, as we expect that people

The associate editor coordinating the review of this article and approving it for publication was Leandro Beltrachini.

This work is licensed under a Creative Commons Attribution 4.0 License. For more information, see http://creativecommons.org/licenses/by/4.0/

close to each other will have similar preferences [3]–[5]. However, although there are many metrics that enable the social closeness between individuals to be measured, it is still unclear which metric is best suited to individual services [6], [7].

Therefore, this paper introduces a new approach based on brain imaging. Brain imaging using functional Magnetic Resonance Imaging (fMRI) is powerful because it enables us to directly observe how a video content stimulates the brains of individual people. We can obtain a personal model from brain imaging data from fMRI and interconnect personal models based on the similarity between them as a network graph. In this paper, we propose an RNP based on similarity of brain activities. We show an application scenario featuring predictive content delivery using the proposed RNP in which, when a user shows interest in a video content in some way, other users close to him or her can be expected to also be interested in it because their brain activities are correlated. Through numerical evaluation using multiple real datasets obtained by fMRI, we demonstrate that the proposed RNP is generalizable across brain imaging results for different sets of video content.

Prior works exist, but their approaches are slightly different. Some brain research has sought to develop methods that characterize individual differences in cognition and behavior by using brain imaging data. Such methods are based, for example, on the representational similarity of object perception [8], the alignment of different brains into a common representational space [9], and brain decoding [10]. However, these methods cannot directly quantify and visualize the relational structure, as represented by a network graph, of personalized brain information. Another line of brain research has applied graph theoretical analysis to brain data [11], [12]. However, network graphs were used only for quantifying anatomical or functional networks between different brain regions, namely, the structural and/or connective characteristics of the brain. The perceptual characteristics of the brain and their individual differences have not been extensively studied from the graph theoretical point of view.

In Section II of this paper, we summarize related work. Section III presents the proposed RNP. Section IV describes the numerical evaluation we performed and reports and discusses the results. We conclude in Section V with a brief summary and mention of future work.

II. RELATED WORK

A. ANALYSIS FOR BRAIN IMAGING

1) REPRESENTATIONAL SIMILARITY ANALYSIS

There has been some past research on representational similarity analysis (RSA) [13]. In RSA, how the brain representations of different entities relate to each other is quantified by the similarity between brain activation patterns evoked by the entities. By examining the similarity structure of activation patterns instead of the activation patterns themselves, RSA enables a direct comparison of brain representations across different representational spaces [9]. Kriegeskorte and colleagues have demonstrated that RSA can be used for the comparison of brain representations between different species [14], the association between brain representations and behaviors [15], and the evaluation of individual differences in brain representations [8].

2) VOXEL-WISE MODELING

Other research has focused on voxel-wise modeling (VM) [16]–[18]. Naselaris et al. proposed a systematic modeling approach that begins by estimating an encoding model for every voxel in a scan and ends by using the estimated encoding models to perform decoding [16]. VM can be used to quantitatively characterize perceptual representations in individual brains from measured brain activity. Accordingly, this method potentially provides a tool to investigate individual differences in brain representations. Huth et al. applied VM to brain activity evoked by natural movies and stories to visualize a representational space of semantic categories in each individual brain [17], [18]. Nishida et al. used VM based on natural language processing features to model each individual brain's structure of semantic representations associated with language [19]. They also developed a decoding method based on the same features to recover the semantic perception of individuals from their fMRI response to natural movies [10].

3) INDIVIDUAL DIFFERENCES

There have also been works on the neural substrates of individual differences in cognitive functions [20]–[24]. These works focused on individual differences particularly in the structural properties of brains and examined their association with the psychological traits of individuals. Dubois and Adolphs discussed issues of validity, reliability, and statistical assessment that arise when the focus shifts to individual subjects and that are applicable also to other imaging modalities [20]. Examining the overall organization of the brain network using graph analysis, Heuvel et al. showed that individual differences in intelligence are strongly associated with those in the path length of functional connections between multiple brain regions [21]. Beaty et al. also utilized graph analysis to identify a brain network associated with individual differences in creative ability [24]. Adelstein et al. reported that five-factor personality traits were mostly associated with brain-regional connections that were inconsistently present across participants [23]. DeYoung et al. also investigated the neural substrates of five-factor personality traits and showed the association of each trait with the volume of different brain regions [22].

B. SOCIAL NETWORK-BASED CONTENT DELIVERY

He and Chu presented a recommender system that can utilize information in social networks, including user preferences, an item's general acceptance, and influence from social friends [3]. They extracted data from a real online social network, and their analysis of a large dataset revealed that friends have a tendency to select the same items and give

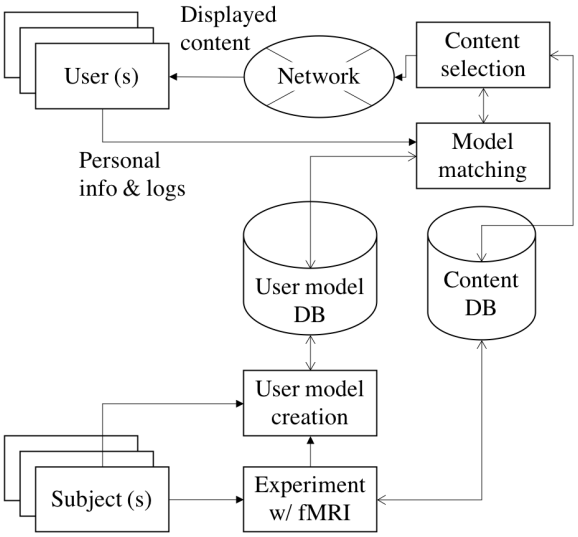

FIGURE 1. Block diagram of system for application scenario example.

similar ratings. They also proposed a way to improve the performance of their system by applying semantic filtering of social networks and validated its improvement through an experiment. Sun et al. proposed a social regularization approach that incorporates social network information to benefit recommender systems [4]. Users' friendships and rating records are utilized to predict the missing values in the user-item matrix. Cui et al. proposed a video recommendation algorithm based on the combination of video content and social network [5]. Their algorithm consists of a trusted friends computing model and a video's quality evaluation model. The former takes into account similarity between users, interaction between users, and the active degree of a user, and the latter combines the acceptance ratio of a video with that video's reputation.

Although the conventional social network represents only whether the established relationship between each pair of people exists or not, there has been much research on ways to develop other social metrics and to differentiate the relationships within a social network. Xiang et al. developed an unsupervised model to estimate relationship strength from interaction activity (e.g., communication, tagging) and user similarity [6]. More specifically, they formulated a link-based latent variable model, along with a coordinate ascent optimization procedure for the inference. Lee and Brusilovsky provided an overview of the technical needs for social link-based recommendations and the studies explaining the viability of users' social networks as useful information sources from a social science point of view [7].

III. PROPOSED RNP

A. APPLICATION SCENARIO EXAMPLE

As mentioned in Section I, one of the killer applications of RNP is the prediction of user demands, which is key to maximizing user satisfaction in content delivery services such as video streaming and video advertising. Figure 1 shows

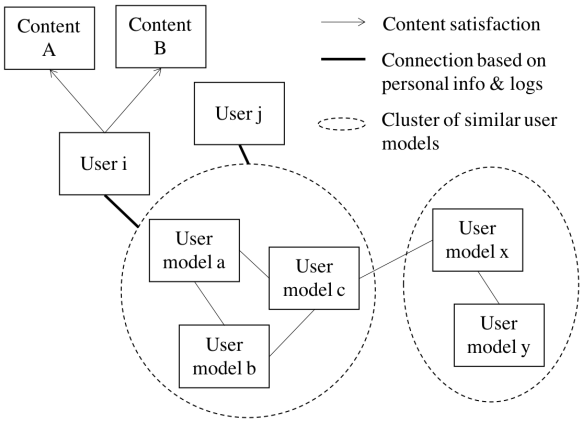

FIGURE 2. RNP-based model used for application scenario example.

a block diagram of the system for the application scenario example. The unidirectional and bidirectional arrows mean the direction of information flow and data reference, respectively. This system consists of users, a network, the content selection part, the model matching part, the user-model database (DB), the content DB, the user-model creation part, the experiment part with fMRI, and subjects. When a user logs in to a Web service, his or her personal information and logs are transferred to the model matching part via the network. According to the information and logs, the model matching part identifies the user model most suitable for that user. Then, the content selection part chooses the best-suited content for the user model from the content DB and predictively delivers it to the user. The usage of the user model in the workflow of the matching part will be explained shortly.

As readers might note, constructing the user-model DB needs to be done beforehand. We recruited as many subjects who contribute to the experiment of brain imaging using fMRI as possible. The user model creation part creates the user models from the brain imaging data obtained from the experiment using fMRI.

Figure 2 shows the RNP-based model used for the application scenario. This model is used by the model matching part in Fig. 1. In this figure, user models created using brain imaging are connected with each other and form clusters with other similar user models. The matching part associates a user with one of the clusters on the basis of his or her personal information and logs. Assuming that users who are associated with the same cluster are likely to be satisfied with the same video content, in the case of the example in the figure, video contents A and B, which were satisfactory for user i, are predictively selected and delivered to user j by the content selection part when he or she logs in to the service.

Considering the real-world applications of the system described above, it would be unrealistic to expect to obtain brain images from all users about all video contents beforehand. Therefore, as a solution, we assume that the system associates a user whose brain-based model has not been obtained yet with the existing brain-based model by using her or his personal information and logs.

B. METHODOLOGY FOR PROPOSED RNP

The technical difficulty in constructing the proposed RNP is that brain imaging signals cannot be directly compared between different people, as the sizes and shapes of brains are different person to person and the brain imaging signals reflect only 'relative' information about brain activities. To solve this problem, we introduce a network graph approach. We first construct the personal model for a subject as the network graph that represents the similarity of brain activities between different video contents. Then, by comparing the personal models of the subjects, we build a network graph that represents the similarity of personal models between subjects. In the numerical evaluation presented in Section IV, we demonstrate that we can generate the proposed RNP across different sets of video content.

We also need to consider how to associate actual users with personal models in the proposed RNP by using their personal information and logs, as in Fig. 2. In the numerical evaluation presented in Section IV, we show that basic personal information such as age, birth location, and so on is not enough for that purpose. Note that identifying the most appropriate personal information and logs for this association are outside the current scope, as this paper focuses on the feasibility of constructing the proposed RNP.

C. PROCEDURE

This section explains the procedure of our RNP, which consists of the following steps.

The brain imaging signal observed when subject i is watching video content c is represented as $v_{i,c}(t)$, which is a multi-dimensional and discrete time function. In general, the number of dimensions of $v_{i,c}(t)$ is too high, so we apply Principal Component Analysis (PCA) [25] to reduce the number of dimensions to k, and thereby obtain $v^k_{i,c}(t)$. When the number of samples of the brain imaging signal in the time dimension is N and the number of dimensions of each brain image is M, we can deal with the brain imaging signal as an $N \times M$ matrix. Then, by using PCA, we can convert the $N \times M$ matrix into an $N \times k$ ($k << M$) matrix.

Next, we calculate the correlation of the brain imaging signals between different video contents. The correlation of the brain imaging signals between video contents $c1$ and $c2$ regarding subject i is represented as $C^k_i(c1, c2)$. When we calculate this, since the lengths of the two video contents can be a little different, Dynamic Time Warping (DTW) [26] is useful to accept such difference. Figure 3 illustrates an example of DTW. We consider the case where the lengths and the number of samples in the time dimension are different between two signals, as shown in Fig. 3(a). DTW determines the optimal time alignment of samples between the two signals that minimizes the total cost. Figure 3(b) illustrates a 'warping path' between the two signals, which represents pairs of indices of samples between the two signals. The optimal path is the one that minimizes the total cost. The absolute difference of values between a pair of samples is used as the cost. Note that, as shown in Fig. 3(a) and (b), multiple samples could be allocated to a sample of the other signal. Thus, DTW enables matching two signals even though their respective lengths and number of samples are different. Then, we obtain the matrix of correlation between video contents for subject i, $\boldsymbol{C}^k_i$. In our RNP, we deal with this as the personal model of subject i; it can be visualized as a network graph in which nodes are video contents and the weight of each link is the correlation of brain imaging signals between the pair of video contents.

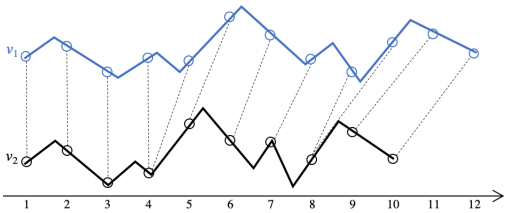

(a) Time alignment between two signals

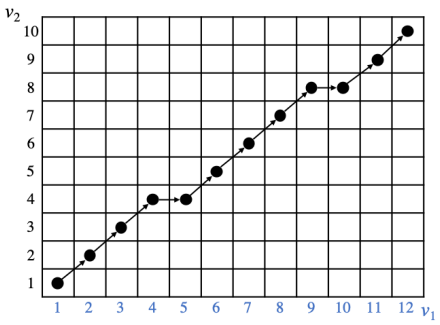

(b) Warping path representing pairs of indices of samples

FIGURE 3. Example of DTW.

The similarity between subjects i and j is measured by the similarity of $\boldsymbol{C}^k_i$ and $\boldsymbol{C}^k_j$, which is calculated by means of the distance between two network graphs in the Weighted Graph Matching Problem (WGMP) [27]. The distance between matrices $\boldsymbol{G}$ and $\boldsymbol{H}$ in WGMP is given as

$$J(\boldsymbol{P}) = |\boldsymbol{P}\boldsymbol{G}\boldsymbol{P}^T - \boldsymbol{H}|^2, \tag{1}$$

where $\boldsymbol{P}$ is called the permutation matrix and $|\cdot|$ is the Euclidean norm. The objective of WGMP is to find the $\boldsymbol{P}$ that minimizes $J(\boldsymbol{P})$. Note that the shorter the distance between two network graphs, the higher the similarity. Finally, we obtain the proposed RNP, in which nodes are subjects and the weight of each link is the distance between the pair of subjects.

IV. NUMERICAL EVALUATION

The objective of the numerical evaluation here is to validate the proposed RNP using real brain imaging datasets. Specifically, we will show that the proposed RNP is generalizable across different sets of content. In addition, we will compare the model created by the proposed RNP with a model created from the basic personal information of subjects. The following sections explain the specifications and setups of the numerical evaluation.

TABLE 1. Basic personal information of subjects.

Item	Description
Gender	2 types
Age	(A) 20-27-48 (B) 21-27-62
Birth month	12 periods
Blood type	4 types
Education	6 types
Handedness	4 types
Birthplace	47 types
Height	(A) 147-166-185 (B) 148-167-185
Weight	(A) 43-56-75 (B) 43-59-88
Residence	47 types
Marital status	2 types
Residential form	8 types
No. of children	5 types
Household income	(A) 0-529-2000 (B) 0-527-2000
Personal annual income	(A) 0-89-650 (B) 0-121-1050
Occupation	15 types
No. of past jobs	6 types
Monthly living expenses	(A) 2-28-300 (B) 2-16-90

TABLE 2. Specifications of video contents used for experiment.

(a) Video setting

File format	avi
Codec	XviD
Frame rate	30 fps
Color mode	YUV 4:2:0 Planar 12 bpp
Rate control	2-pass fixed bit rate
Bit rate	10,000 kbps
Display mode	Progressive
Aspect ratio	16:9
Filtering	Cropping & padding if necessary

(b) Audio setting

Codec	PCM signed 16-bit Little-Endian 1411 kbps
Sampling	44100 Hz
No. of channels	2-ch (stereo)
Volume	Normalized to 89 dB

A. SUBJECTS

We utilized two subject groups: A, consisting of 27 subjects, and B, consisting of 40. A questionnaire was administered to obtain their basic personal information, the items and answers of which are listed in Table 1. In the table, if the form of an answer is a value, the minimum, average, and maximum in groups A and B are listed. The nationality of all subjects was Japanese. We recruited the subjects from among members of the public in a local area close to the experimental facility of an MRI scanner, which is in Suita-city, Osaka, Japan. As seen in Table 1, the basic personal information of subjects varied significantly, particularly in terms of age, income, and expenses.

B. VIDEO CONTENTS

The specifications of the video contents used for the evaluation are summarized in Table 2 and the description is provided in Table 3. We used video content datasets that were broadcast as TV or online advertising materials. As shown in Table 3, the video contents we used also varied widely in terms of period and category. Thus, by using a wide variety of video contents (as explained here) and by recruiting a wide variety of subjects (as explained earlier), we eliminated potential bias of video contents on subjects.

TABLE 3. Description of video contents used for experiment.

	Group A	Group B
No. of short videos	240 (15 sec)	153 (14 to 24 sec)
No. of long videos	120 (30 sec)	161 (25 to 44 sec)
Broadcasting region	Japan	Japan
Broadcasting period	July 2011 to Dec. 2017	July 2015 to March 2017
Food / fast food	91	23
Medical / cosmetic / daily products	53	69
Appliances / cars / long-term use products	99	105
Communication / games / distribution, retailing services	117	119

TABLE 4. Specifications of fMRI scanning.

Parameters	Value
Repetition time	1000 ms
Echo time	30 ms
Flip angle	60°
Voxel size	$2 \times 2 \times 2$ mm
Matrix size	96×96
No. of axial slices	72
Multiband factor	6

C. EXPERIMENT USING FMRI

A 3T Siemens MAGNETOM Prisma scanner (Siemens, Germany) was used with a 32-channel Siemens volume coil and a multiband gradient echo-EPI sequence [28]. The specifications of the fMRI scanning are listed in Table 4. The field of view covered the entire cortex. Anatomical data were also collected using a T1-weighted MPRAGE sequence on the same 3T scanner. The experimental protocol was approved by the ethics and safety committees of the National Institute of Information and Communications Technology.

In the experiments, subjects viewed the movie stimuli on a projector screen inside the scanner ($27.9° \times 15.5°$ of visual angle) and listened to the audio stimuli through MR-compatible headphones. The subjects were given no explicit task. The fMRI response data from individual subjects were collected in three separate recording sessions over three days.

To create the movie stimuli, original ad movies were sequentially concatenated in a pseudo-random order. Fourteen non-overlapping movie clips 610 s in length were obtained. The individual movie clips were displayed in separate scans. The initial 10-s part of each clip was a dummy to discard hemodynamic transients caused by clip onset. fMRI responses collected during the 10-s dummy movie were not used for the analysis. Twelve of the clips were presented once each and the other two clips were presented four times each in four separate scans. fMRI response to these two clips were averaged across the four scans.

For preprocessing of the fMRI data, motion correction in each functional scan was performed using the Statistical

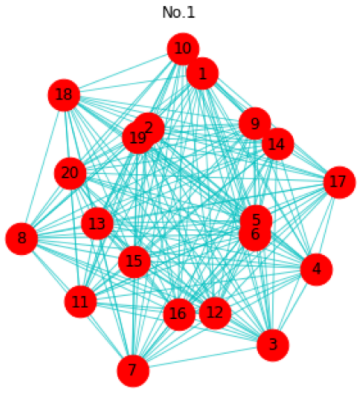

FIGURE 4. Personal model of ID01 in group A (1000 dimensions).

Parameter Mapping toolbox (SPM8) [29]. All volumes were aligned to the first image from the first functional run for each subject. Low-frequency fMRI response drift was detected using a median filter with a 120-s window and subtracted from the signal. The response for each voxel was then normalized by subtracting the mean response and scaling it to the unit variance. FreeSurfer [30], [31] was used to identify cortical surfaces from anatomical data and register them to the voxels of functional data. All voxels identified within the whole cortex for each subject were used for the analysis.

D. TOOLS

Our numerical evaluation followed the procedure of the proposed RNP described in Section III-C. We used the following tools for PCA, DTW, and Graph Visualization.

- PCA by scikit-learn [32]
- DTW by Python library [33]
- Graph visualization by Networkx [34]

E. RESULTS OF CORRELATION BETWEEN DISTANCE MATRICES

Figure 4 shows the visualized personal model of subject ID01 in group A as an example of the personal model. In this case, the number of dimensions of PCA, k, was set to 1000. As explained in Section III-C, the personal model of a subject is the matrix of correlations of brain imaging signals between video contents for the subject. In Fig. 4, the matrix is represented as a network graph in which nodes are video contents, while the values of correlations between them are set as the weights of links. That is, video contents close to each other in this network graph visualization have a large correlation between them for that subject.

Figure 5 shows the personal models of all subjects in group A. Although we do not explain the details subject by subject, the variety of personal models is roughly visualized in this figure.

Next, we show the visualization of the matrix of the distance between subjects for short and long videos in Fig. 6(a) and (b). As shown, the distribution of distances between subjects ranged from around 5 to 15. To investigate the distributions of distances between subjects in other cases of the number of dimensions of PCA, groups, and video lengths, we summarize the average and the standard deviation of distance between subjects in Tables 5 and 6.

To validate the proposed RNP created using the brain imaging datasets of groups A and B, we calculated the correlation coefficient of distance matrices between short and long videos, which is shown in Table 7. As shown, the correlation was larger than 0.9 for all cases of the number of dimensions of PCA and groups. We can see the correlation for group A from the visual comparison between Fig. 6(a) and (b). This suggests that the proposed RNP is generalizable across different sets of video contents by our methodology. Thus, brain imaging data can be used to robustly generate RNP that can be utilized as a powerful tool for estimating user preferences.

F. RESULTS OF CORRELATION BETWEEN DISTANCE MATRIX AND BASIC PERSONAL INFORMATION

Next, we investigate the correlation between the distance matrix and the basic personal information we obtained from the questionnaire (listed in Table 1). To create the distance matrix from the basic personal information, we calculated

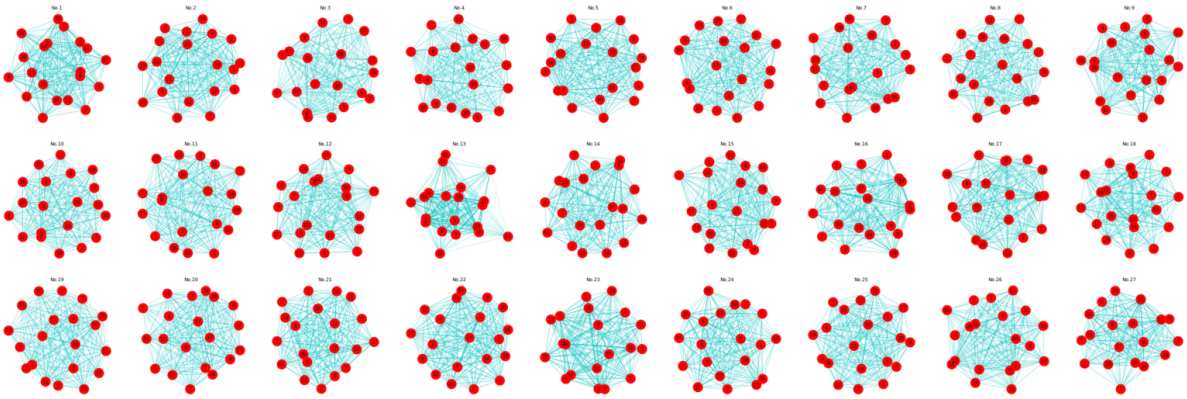

FIGURE 5. Personal models of all subjects in group A (1000 dimensions).

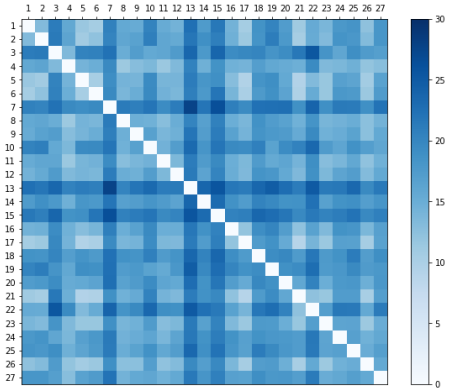

(a) Short videos

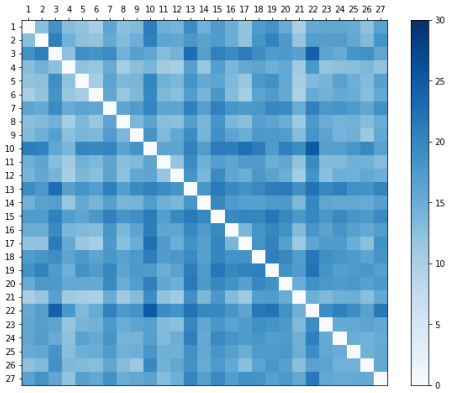

(b) Long videos

FIGURE 6. Distance matrix of subjects in group A (1000 dimensions).

TABLE 5. Average and standard deviation of distance between subjects (group A).

(a) Short videos

No. of dimensions	Avg.	Standard dev.
500	18.04	3.62
1000	17.34	3.49
2000	16.53	3.35
4000	15.78	3.29

(b) Long videos

No. of dimensions	Avg.	Standard dev.
500	16.91	2.82
1000	16.4	2.8
2000	15.84	2.79
4000	15.37	2.87

the Hamming distance of the answers between each pair of subjects. However, if the form of an answer was a value, we converted it to a categorical variable. The step sizes of age, height, weight, household income, personal annual income, and monthly living expenses in Table 1 were set to 5, 5, 5, 100, 100, and 5, respectively. The results are shown in Table 8 (a) and (b). As shown, the correlation coefficient was smaller than around 0.15, which suggests that the proposed RNP is quite different from the one constructed

TABLE 6. Average and standard deviation of distance between subjects (group B).

(a) Short videos

No. of dimensions	Avg.	Standard dev.
500	18.37	3.54
1000	17.83	3.54
2000	17.16	3.48
4000	16.50	3.52

(b) Long videos

No. of dimensions	Avg.	Standard dev.
500	16.26	3.58
1000	15.75	3.53
2000	15.20	3.39
4000	14.74	3.38

TABLE 7. Correlation coefficient of distance matrices between short and long videos.

No. of dimensions	Group A	Group B
500	0.917	0.916
1000	0.920	0.920
2000	0.928	0.926
4000	0.938	0.934

TABLE 8. Correlation coefficient between distance matrix and basic personal information.

(a) Group A

No. of dimensions	Short video	Long video
500	0.1536	0.0833
1000	0.1356	0.0741
2000	0.1076	0.0655
4000	0.0827	0.0696

(b) Group B

No. of dimensions	Short video	Long video
500	-0.1328	-0.1570
1000	-0.1291	-0.1502
2000	-0.1249	-0.1414
4000	-0.1072	-0.1103

in the conventional way that uses only the basic personal information of individuals.

V. CONCLUSION

In this paper, we have proposed a brain imaging-based RNP that represents the similarity of brain activities between individuals as a network graph. We showed an application scenario featuring predictive content delivery using the proposed RNP in which, when a user shows interest in a video content in some way, it is predicted that other users close to him or her will also be interested in it because their brain activities are correlated. Through numerical evaluation using multiple real datasets obtained by fMRI, we demonstrated that the proposed RNP can be identically created from brain imaging results for different sets of video content. Thus, brain imaging data can be used to robustly generate RNP that can be utilized as a powerful tool for estimating user preferences. Future work includes further development of RNP and its association with personal information and logs to make it more effective for the predictive content delivery scenario discussed in Section III-A. Readers may be interested in the similarity or correlation analysis of the proposed RNP with respect to how

familiar people are to each other, which this paper did not show and will be also included in future work.

ACKNOWLEDGMENT

The authors would like grateful to Mr. Fumihiro Takayama and Mr. Yoshifumi Aimoto of NTT DATA Institute of Management Consulting, Inc. for sharing datasets for this work. They also thank Mr. Yuichi Inagaki, Mr. Keiichiro Sato, and Mr. Shuichirou Shimizu, who are students at Kyoto University, for their assistance.

REFERENCES

[1] R. Shinkuma, Y. Sugimoto, and Y. Inagaki, "Weighted network graph for interpersonal communication with temporal regularity," *Soft Comput.*, vol. 23, no. 9, pp. 3037–3051, May 2019.

[2] *Video Streaming (SVoD)*. Accessed: Apr. 25, 2019. [Online]. Available: https://www.statista.com/

[3] J. He and W. W. Chu, "A social network-based recommender system (SNRS)," in *Data Mining for Social Network Data* (Annals of Information Systems), vol. 12. Boston, MA, USA: Springer, 2010, pp. 47–74.

[4] Z. Sun, L. Han, W. Huang, X. Wang, X. Zeng, M. Wang, and H. Yan, "Recommender systems based on social networks," *J. Syst. Softw.*, vol. 99, pp. 109–119, Jan. 2015.

[5] L. Cui, L. Dong, X. Fu, Z. Wen, N. Lu, and G. Zhang, "A video recommendation algorithm based on the combination of video content and social network," *Concurrency Comput., Pract. Exper.*, vol. 29, no. 14, Jul. 2017, Art. no. e3900.

[6] R. Xiang, J. Neville, and M. Rogati, "Modeling relationship strength in online social networks," in *Proc. 19th Int. Conf. World Wide Web*, Apr. 2010, pp. 981–990.

[7] D. Lee and P. Brusilovsky, "Recommendations based on social links," in *Social Information Access* (Lecture Notes in Computer Science), vol. 10100. Cham, Switzerland: Springer, 2018, pp. 391–440.

[8] I. Charest, R. A. Kievit, T. W. Schmitz, D. Deca, and N. Kriegeskorte, "Unique semantic space in the brain of each beholder predicts perceived similarity," *Proc. Nat. Acad. Sci. USA*, vol. 111, no. 40, pp. 14565–14570, Oct. 2014.

[9] N. Kriegeskorte, M. Mur, and P. Bandettini, "Representational similarity analysis—Connecting the branches of systems neuroscience," *Frontiers Syst. Neurosci.*, vol. 2, no. 4, Nov. 2008, p. 4.

[10] S. Nishida and S. Nishimoto, "Decoding naturalistic experiences from human brain activity via distributed representations of words," *NeuroImage*, vol. 180, pp. 232–242, Oct. 2018. doi: 10.1016/j.neuroimage.2017.08.017.

[11] E. Bullmore and O. Sporns, "Complex brain networks: Graph theoretical analysis of structural and functional systems," *Nature Rev. Neurosci.*, vol. 10, no. 3, pp. 186–198, Mar. 2009.

[12] D. S. Bassett and O. Sporns, "Network neuroscience," *Nature Neurosci.*, vol. 20, no. 3, pp. 353–364, Feb. 2017.

[13] N. Kriegeskorte and R. A. Kievit, "Representational geometry: Integrating cognition, computation, and the brain," *Trends Cognit. Sci.*, vol. 17, no. 8, pp. 401–412, Aug. 2013. doi: 10.1016/j.tics.2013.06.007.

[14] N. Kriegeskorte, M. Mur, D. A. Ruff, R. Kiani, J. Bodurka, H. Esteky, K. Tanaka, and P. A. Bandettini, "Matching categorical object representations in inferior temporal cortex of man and monkey," *Neuron*, vol. 60, no. 6, pp. 1126–1141, Dec. 2008. doi: 10.1016/j.neuron.2008.10.043.

[15] M. Mur, M. Meys, J. Bodurka, R. Goebel, P. A. Bandettini, and N. Kriegeskorte, "Human object-similarity judgments reflect and transcend the primate-IT object representation," *Frontiers Psychol.*, vol. 4, p. 128, Mar. 2013. doi: 10.3389/fpsyg.2013.00128.

[16] T. Naselaris, K. N. Kay, S. Nishimoto, and J. L. Gallant, "Encoding and decoding in fMRI," *NeuroImage*, vol. 56, no. 2, pp. 400–410, May 2011. doi: 10.1016/j.neuroimage.2010.07.073.

[17] A. G. Huth, S. Nishimoto, A. T. Vu, and J. L. Gallant, "A continuous semantic space describes the representation of thousands of object and action categories across the human brain," *Neuron*, vol. 76, no. 6, pp. 1210–1224, Dec. 2012. doi: 10.1016/j.neuron.2012.10.014.

[18] A. G. Huth, W. A. de Heer, T. L. Griffiths, F. E. Theunissen, and J. L. Gallant, "Natural speech reveals the semantic maps that tile human cerebral cortex," *Nature*, vol. 532, no. 7600, pp. 453–458, Apr. 2016. doi: 10.1038/nature17637.

[19] S. Nishida, A. G. Huth, J. L. Gallant, and S. Nishimoto, "Word statistics in large-scale texts explain the human cortical semantic representation of objects, actions, and impressions," in *Proc. Soc. Neurosci. Annu. Meeting*, Oct. 2015, vol. 333, no. 13.

[20] J. Dubois and R. Adolphs, "Building a science of individual differences from fMRI," *Trends Cognit. Sci.*, vol. 20, no. 6, pp. 425–443, Jun. 2016. doi: 10.1016/j.tics.2016.03.014.

[21] M. P. van den Heuvel, C. J. Stam, R. S. Kahn, and H. E. H. Pol, "Efficiency of functional brain networks and intellectual performance," *J. Neurosci.*, vol. 29, no. 23, pp. 7619–7624, Jun. 2009. doi: 10.1523/jneurosci.1443-09.2009.

[22] C. G. DeYoung, J. B. Hirsh, M. S. Shane, X. Papademetris, N. Rajeevan, and J. R. Gray, "Testing predictions from personality neuroscience: Brain structure and the big five," *Psychol. Sci.*, vol. 21, no. 6, pp. 820–828, Jun. 2010. doi: 10.1177/0956797610370159.

[23] J. S. Adelstein, Z. Shehzad, M. Mennes, C. G. DeYoung, X.-N. Zuo, C. Kelly, D. S. Margulies, A. Bloomfield, J. R. Gray, F. X. Castellanos, and M. P. Milham, "Personality is reflected in the brain's intrinsic functional architecture," *PLoS ONE*, vol. 6, no. 11, Nov. 2011, Art. no. e27633. doi: 10.1371/journal.pone.0027633.

[24] R. E. Beaty, Y. N. Kenett, A. P. Christensen, M. D. Rosenberg, M. Benedek, Q. Chen, A. Fink, J. Qiu, T. R. Kwapil, M. J. Kane, and P. J. Silvia, "Robust prediction of individual creative ability from brain functional connectivity," *Proc. Nat. Acad. Sci. USA*, vol. 115, no. 5, pp. 1087–1092, Jan. 2018. doi: 10.1073/pnas.1713532115.

[25] C. G. Thomas, R. A. Harshman, and R. S. Menon, "Noise reduction in BOLD-based fMRI using component analysis," *NeuroImage*, vol. 17, no. 3, pp. 1521–1537, Nov. 2002.

[26] M. Müller, "Dynamic time warping," in *Information Retrieval for Music and Motion*. Berlin, Germany: Springer-Verlag, 2007, pp. 69–84.

[27] S. Umeyama, "An eigendecomposition approach to weighted graph matching problems," *IEEE Trans. Pattern Anal. Mach. Intell.*, vol. 10, no. 5, pp. 695–703, Sep. 1988.

[28] S. Moeller, E. Yacoub, C. A. Olman, E. Auerbach, J. Strupp, N. Harel, and K. Uğurbil, "Multiband multislice GE-EPI at 7 tesla, with 16-fold acceleration using partial parallel imaging with application to high spatial and temporal whole-brain fMRI," *Magn. Reson. Med.*, vol. 63, no. 5, pp. 1144–1153, May 2010. doi: 10.1002/mrm.22361.

[29] University College, London, U.K., 2009. *Statistical Parametric Mapping (SPM) Version 8*. Accessed: Apr. 25, 2019. [Online]. Available: http://www.fil.ion.ucl.ac.uk/spm/software/spm8/

[30] A. M. Dale, B. Fischl, and M. I. Sereno, "Cortical surface-based analysis. I. Segmentation and surface reconstruction," *NeuroImage*, vol. 9, no. 2, pp. 179–194, 1999. doi: 10.1006/nimg.1998.0395.

[31] B. Fischl, M. I. Sereno, and A. M. Dale, "Cortical surface-based analysis: II: Inflation, flattening, and a surface-based coordinate system," *NeuroImage*, vol. 9, no. 2, pp. 195–207, Feb. 1999. doi: 10.1006/nimg.1998.0396.

[32] *Scikit-Learn: Machine Learning in Python*. Accessed: Apr. 25, 2019. [Online]. Available: https://scikit-learn.org/stable/

[33] *DTW (Dynamic Time Warping) Python Module*. Accessed: Apr. 25, 2019. [Online]. Available: https://github.com/pierre-rouanet/dtw

[34] *Overview of NetworkX*. Accessed: Apr. 25, 2019. [Online]. Available: https://networkx.github.io/documentation/stable/

RYOICHI SHINKUMA (S'02–M'03–SM'19) received the B.E., M.E., and Ph.D. degrees in communications engineering from Osaka University, Japan, in 2000, 2001, and 2003, respectively. In 2003, he joined the Faculty of Communications and Computer Engineering, Graduate School of Informatics, Kyoto University, Japan, where he is currently an Associate Professor. He was a Visiting Scholar with the Wireless Information Network Laboratory, Rutgers, the State University of New Jersey, USA, from 2008 to 2009. His research interest is mainly cooperation in heterogeneous networks. He received the Young Researchers' Award from IEICE, in 2006, and the Young Scientist Award from Ericsson Japan, in 2007. He also received the Telecom System Technology Award from the Telecommunications Advancement Foundation, in 2016, and the Best Tutorial Paper Award from the IEICE Communications Society, in 2019. He was the Chairperson of the Mobile Network and Applications Technical Committee of the IEICE Communications Society, from 2017 to 2019.

SATOSHI NISHIDA received the Ph.D. degree in medicine from Kyoto University, Japan, in 2014. After short-term postdoctoral work at Kyoto University, he joined CiNet, NICT, Japan, in 2014, where he is currently a Senior Researcher. Since 2015, he has been a Visiting Researcher with the Graduate School of Frontier Biosciences, Osaka University, Japan. His current research interests include the areas of cognitive neuroscience, experimental psychology, and artificial intelligence. He received the Young Researcher Award from the IEEE CIS Japan Chapter, in 2011, and the Best Research Award from the Japan Neural Network Society, in 2011.

MASATAKA KADO has been with NTT DATA Corporation, since 2003. He was involved in research and development on network security and the cloud, from 2003 to 2010 and involved in applied research on advanced technologies relating to neuroscience and human sensing, from 2011 to 2015. Since 2016, he has been working on the planning and commercialization of neurobusiness.

NAOYA MAEDA joined the Software House as a new graduate, in 1997, where he was involved in system development for the telecom, engineering, entertainment, medical, and research industries. In 2005, he joined NTT DATA, where he was involved in project management for corporate system development and business support by customer residency. Since 2014, he has been working on applied research and commercialization of integrated neuroscience and artificial intelligence technology through industry-academia collaboration.

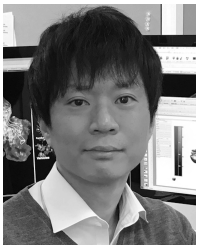

SHINJI NISHIMOTO received the Ph.D. degree in neurophysiology from Osaka University, Japan, in 2005. He was a Postdoctoral Fellow and an Associate Specialist with the Helen Wills Neuroscience Institute, University of California, Berkeley, from 2005 to 2013. He joined CiNet with the National Institute of Information and Communications Technology (NICT), as a Senior Researcher (Principal Investigator). He has also been affiliated as the Guest Professor with the Graduate School of Medicine and the Graduate School of Frontier Biosciences, Osaka University. His research interest includes the quantitative understanding of neural computation and representation. He received Time Magazine's 50 Best Inventions of 2011 and Ichimura Prize in Science for Distinguished Achievement, in 2017.